Corrosion Science 141 (2018) 221–229

Contents lists available at ScienceDirect

Corrosion Science

journal homepage: www.elsevier.com/locate/corsci

Chloride-induced corrosion behavior of cold-drawn pearlitic steel wires

Song Xiang[a,b,c,*], Yue He[a], Wei Shi[a,b,*], Xuanming Ji[a,b], Yuanbiao Tan[a,b], Jianmin Liu[a], Ronald G. Ballinger[c]

[a] College of Materials and Metallurgy, Guizhou University, Guiyang 550025, China
[b] Key Laboratory for Mechanical Behavior and Microstructure of Materials of Guizhou Province, Guizhou University, Guiyang 550025, China
[c] H.H. Uhlig Corrosion Laboratory, Massachusetts Institute of Technology, Cambridge, MA 02139, United States

ARTICLE INFO

Keywords:
Pearlitic steel wires
Corrosion behavior
LEIS
TEM
APT

ABSTRACT

The chloride induced corrosion behavior of cold drawn pearlitic steel wires was systematically investigated using electrochemical measurements, namely, electrochemical impedance spectroscopy, and local electrochemical impedance spectroscopy for micro-areas. A 0.05 mol/L NaCl solution mixed with borate buffer solution (pH = 8.45) was used. The results suggest that the corrosion resistance of cold-drawn pearlitic steel decreases with increasing strain to 0.8, but increases with strain up to a value of 1.6. Microstructure evolution was characterized by electron back scatter diffraction in combination with scanning electron microscopy and transmission electron microscopy. Atom probe tomography was used to quantify the cementite decomposition. The quantitation of microstructural parameters with strain suggests that the evolution of defect structure markedly increases the corrosion susceptibility of pearlite for strain up to 0.8. In the case of strain 1.6, refinement of the lamellar structure and cementite decomposition can reduce the volume fraction of cementite that acts as the cathode per corrosion unit (a pearlite/cementite "cell"), giving rise to an increase in the corrosion resistance.

1. Introduction

Cold drawn pearlitic steel wires have generally attracted marked interest because of their excellent combination of strength and ductility [1]. Numerous research results provided detailed characterization of microstructural evolution by using systematic electron microscopy techniques [2–4]. Deformation of pearlite during cold drawing is approximately divided into two different stages; that is, below a strain of approximately 1.5, the refinement and reorientation of cementite lamellae with respect to the drawing direction are the main features. At higher strains, decomposition of the cementite lamellae starts to occur accompanied by continuous refinement [5–8]. The corresponding strengthening mechanisms and strength–structure relationships were proposed in Ref. [9–11].

For marine steel wires, which are widely applied in marine and offshore structures, corrosion is a primary cause of structural deterioration [12]. However, minimal attention has been focused to the corrosion behavior of cold-drawn pearlitic steel wires. Using atomic force microscopy (AFM), Sánchez et al. [13] found that the morphology of high strength steel wires exposed in a diluted sodium chloride solution exhibited a typical pearlitic microstructure, which suggests a preferential attack of ferrite, whereas cementite acts as the cathode. The existence of cementite was shown by Hao et al. [14] to be harmful to the corrosion resistance of steels because the cementite area accumulates continuously on the surface to enhance galvanic corrosion when ferrite is preferentially dissolved. Rault et al. [15] found that when coupled with brass, pearlitic steel shows increased corrosion rate in sodium chloride solution after plastic deformation; this phenomenon was believed to be due to the fine microstructure and high density of dislocations induced by cold drawing. Thus, whether and how the change in microstructural parameters induced by cold drawing influences the corrosion resistance of pearlitic steel remain unclear. In particular, whether cementite decomposition affects the corrosion resistance of pearlitic steel is still unknown.

This work aims to explore the relationship between the corrosion behavior and the microstructural parameters of pearlitic steels during cold drawing. In particular, the corrosion behavior of pearlitic steels was studied by observing and analyzing the evolution of corrosion morphology in chloride-containing aqueous environments by using electrochemical measurements, namely, electrochemical impedance spectroscopy (EIS), potentiodynamic scan, and local electrochemical impedance spectroscopy (LEIS) for micro-areas. The evolution of

* Corresponding authors at: College of Materials and Metallurgy, Guizhou University, Guiyang 550025, China.
E-mail addresses: sxiang@gzu.edu.cn (S. Xiang), wshi@gzu.edu.cn (W. Shi).

https://doi.org/10.1016/j.corsci.2018.07.015
Received 17 May 2017; Received in revised form 15 June 2018; Accepted 6 July 2018
Available online 17 July 2018
0010-938X/

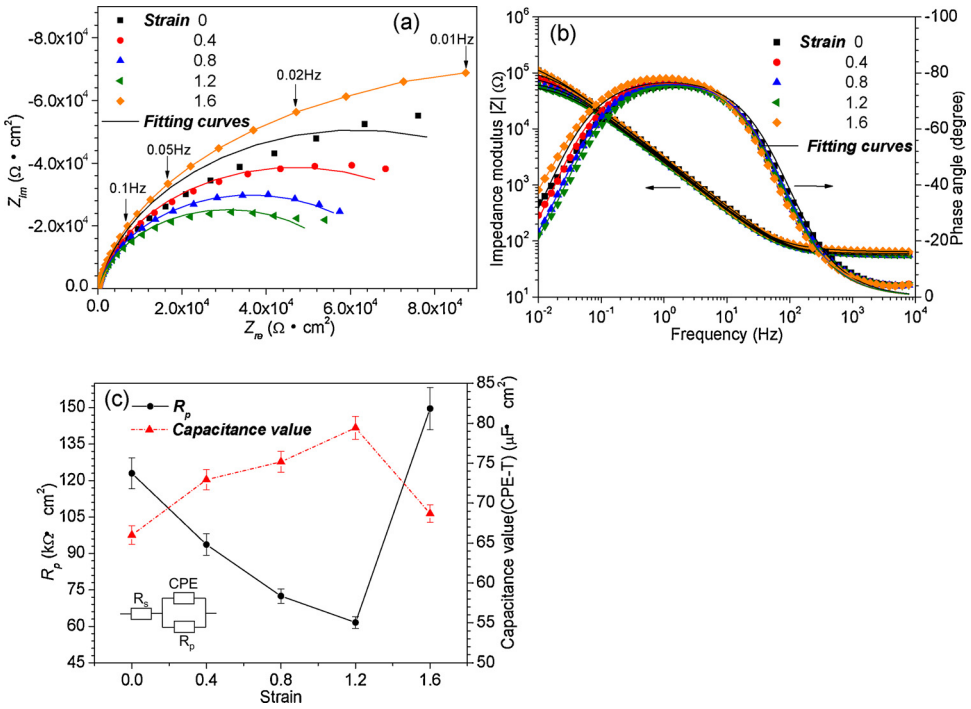

Fig. 1. EIS diagrams showing cold drawn pearlitic steels at different strains: Nyquist representation (a), Bode representation (b), calculated polarization resistance, and capacitance value (c) obtained from equivalent circuit that describes the steel–solution interface.

microstructure evolution was characterized by electron back-scatter diffraction (EBSD) in combination with scanning electron microscopy (SEM) and transmission electron microscopy (TEM). Atom probe tomography (APT) was used to quantify the behavior of cementite decomposition. The experimental quantification serves as the basis for further discussion on the influence of microstructural parameters on corrosion behavior.

2. Experimental

2.1. Materials

The materials studied in this paper are pearlitic steel wires, with the chemical composition of Fe–0.81C–0.22Si–0.77 Mn (wt. %), which were provided by Guizhou Wire Rope Incorporated Corporation. The rods were hot rolled at temperature ranging from 940 to 1050 centigrade before air cooling. After pickling with hydrochloric acid and phosphating, hot-rolled steel rods (12.5 mm in diameter) were drawn successively to a final diameter of 5.56 mm. The drawing speed of the cold drawing was lower than 15 m/s. Samples with $\varepsilon = 0$ (12.5 mm in diameter), $\varepsilon = 0.4$ (10.46 mm in diameter), $\varepsilon = 0.8$ (8.35 mm in diameter), $\varepsilon = 1.2$ (6.76 mm in diameter), and $\varepsilon = 1.6$ (5.56 mm in diameter) were obtained at intermediate steps in the drawing process.

By using wire cut electric discharge machine, the samples were obtained from the longitudinal section. Samples were cut at each strain with length, width, and thickness values of 5, 4.5, and 2 mm, respectively, from the longitudinal section. Prior to the measurements, the samples were wet-ground with SiC papers of 400, 800, 1200, and 2000 grit size, polished with a 1 μm diamond spray, cleaned in deionized water, and degreased in ethanol.

2.2. Electrochemical measurements

We applied a classical three-electrode cell, with a saturated calomel electrode (SCE) acting as reference electrode and a platinum foil as counter electrode, whereas the samples with diverse strains were used as working electrodes (WEs). To control the degree of corrosion at a reasonable state to distinguish the difference of corrosion morphology clearly, we used a 0.05 mol/L NaCl solution mixed with borate buffer solution (pH = 8.45) was used [16]. For achieving a steady-state condition, the samples were immersed in the solution for 30 min before the open circuit potential value tended toward stability. Then, the EIS measurements were carried out at the open circuit potential with a perturbation amplitude of 10 mV in a frequency range of 10^5 Hz to 10^{-2} Hz at room temperature.

LEIS behavior was measured on the WEs using a BioLogic Model 370 scanning electrochemical workstation. The step length of the LEIS scanning was 15.625 μm, and the measuring frequency was fixed at 10 kHz.

2.3. Microstructure characterization and corrosion morphology observation

The microstructure evolution of the etched samples was characterized by standard visual techniques, such as SEM (ZEISS SUPRA40) and TEM (JEM-1200EX, Tecnai G2 F20 S-TWIN). The interlamellar spacing (ILS) and cementite lamella thickness (t) were measured by TEM, taking care to ensure edge-on conditions to determine cementite lamella thickness(t) [9]. To measure EBSD, the samples were electropolished with perchlorate alcohol solution, and the morphological observations of electron channeling contrast (ECC) were carried out by using an electron back scattering probe. Moreover, ferrite orientation was characterized by the HKL channel 5 EBSD from Oxford Instruments. Samples were immersed in the solution for seven days before observation.

2.4. Atomic probe tomography

A local electrode atom probe (LEAP 4000 HR, Cameca Instrument) was used to quantify the behavior of cementite dissolution. Needle-shaped samples with the tips perpendicular to the wire axis were prepared by the standard electropolishing procedure, and APT analyses were performed according to the description in previous studies [17–19].